Slip acceleration generates seismic tremor like signals in friction experiments

Dimitri Zigone, Christophe Voisin, Éric Larose, Francois Renard, Michel Campillo

Slip Acceleration Generates Seismic Tremor Like Signals in Friction Experiments

Zigone, D[1], C. Voisin[2,3], E. Larose[1], F. Renard[4,5], and M. Campillo[1]

[1] Laboratoire de Géophysique Interne et Tectonophysique, CNRS, Université Joseph Fourier, Maison des Géosciences, BP 53, 38041 Grenoble, France
[2] Laboratoire de Géophysique Interne et Tectonophysique, IRD, CNRS, Université Joseph Fourier, Maison des Géosciences, BP 53, 38041 Grenoble, France
[3] CNRSL, Centre de Recherches Géophysiques, Bhannès, Liban
[4] Laboratoire de Géodynamique des Chaînes Alpines, CNRS, Université Joseph Fourier, Maison des Géosciences, BP 53, 38041 Grenoble, France
[5] Physics of Geological Processes, University of Oslo, Norway

Since their discovery nearly a decade ago, the origin of seismic tremor remains unclear. Recent studies indicate that various driving phenomena such as Earth and ocean tides, regional and teleseismic earthquakes enhance tremor activity. Observations of the coincidence with slow-slip events and of fast migrations of tremors have led frictional slip to be considered as the possible source of tremors. Indeed, laboratory friction experiments succeeded in generating and recording tremor like signals (TLS). Here we show a systematic correlation between the onset of slip acceleration and the emission of TLS in a laboratory friction experiment. TLS are generated when the shear stress reaches the peak static resistance and the dilatancy meets its maximum that is when the mature interface is close to failure. This robust result provides a comprehensive image of how natural seismic tremors might be generated and/or triggered by passing seismic waves, tides or even slow slip events.

Introduction:

Seismic tremors, named also non-volcanic tremors, have now been well documented and studied in many subduction zones [*Dragert et al.*, 2004; *Hirose and Obara*, 2006; *Kao et al.*, 2005; *Obara*, 2002; *Obara and Hirose*, 2006; *Shelly et al.*, 2007b; *Shelly et al.*, 2006] and along some continental fault segments [*Ghosh et al.*, 2009b; *Nadeau and Dolenc*, 2005; *Peng et al.*, 2009; *Peng et al.*, 2008]. Recent studies indicate that various driving phenomena such as Earth and ocean tides [*Thomas et al.*, 2009], regional and teleseismic earthquakes [*Ghosh et al.*, 2009b; *Peng et al.*, 2009; *Peng et al.*, 2008; *Rubinstein et al.*, 2009] enhance tremor activity. Frictional slip was proposed as the possible source of tremors [*Brown et al.*, 2009; *Ghosh et al.*, 2009a; *Ide et al.*, 2007; *Kao et al.*, 2007; *La Rocca et al.*, 2009; *Larmat et al.*, 2009]**.**

Laboratory experiments specifically designed to study seismic tremors are a powerful tool to explore the physical processes at the origin of these signals. Few experiments have been successful in producing tremor like signals (TLS) so far. They involve fluid-flow and fluid processes [*Burlini et al.*, 2009], or frictional processes associated with shear of a deformable sample [*Voisin et al.*, 2007; *Voisin et al.*, 2008]. Our experimental setup (Fig. 1A) is designed to reproduce different frictional behaviors, from stick-slip to stable sliding. We make use of a deformable slider of salt (NaCl) pushed at constant load-point velocity, under constant conditions of normal pressure (0.26 MPa), temperature (22°C) and ambient humidity. Using a salt slider allows for the brittle and ductile deformation to be effective on the time scale of our experiments, aimed to serve as an analogue for natural faults deforming in the brittle and ductile regimes at 20-40 km depth. We continuously record the frictional force and the acoustic emission generated during the shear of the sample. These signals are carefully scrutinized in order to investigate the temporal timing of the sliding characteristics and of the TLS emission.

Results:

Figure 1 (B, C, D), presents three different stages of a friction experiment representative of the stable, intermediate and unstable frictional regimes. The unstable regime is characterized by cycles of long stress increase followed by sudden drops of the friction force, associated with the stick-slip behavior of the slider (stage 1, Fig. 1B). The jumps of the slider produce short duration and high amplitude acoustic signals. In this stage of stick-slip, no TLS is recorded. The salt slider follows an evolution from an unstable stick-slip behavior to more and more stable behavior with accumulated displacement [*Voisin et al.*, 2007]. Figure 1C presents a second experiment (under the same conditions) where the sample has accumulated 3.3 mm of displacement and for which the slider interface has become more mature (stage 2). In this condition, the stick-slip behavior changes and smoothens. The slider still obeys a stick-slip behavior, but is creeping before and after the jump. Interestingly, the associated acoustic emission presents two types of signals: i) a tremor like signal with long duration and low amplitude followed by ii) a strong impulsive and short duration event, signature of the jump. Finally, Figure 1D presents an experiment in the stable regime, characterized by smooth oscillations of the frictional force around a mean value, which corresponds to smooth variations of the sliding velocity of the slider [*Voisin et al.*, 2007]. During this stable regime, the acoustic emission is composed exclusively of noise and TLS. Those TLS are identical to those presented in Figure 1C in terms of frequency content, duration and amplitude,

suggesting their common physical origin. These results show that TLS in friction experiments are related to regimes of stable slip (Fig 1D) or simultaneous creep and stick-slip (Fig 1C). Note however, that the high level of experimental noise impairs to exclude definitively the existence of TLS at other time than the slip events.

Figure 2 presents 4 typical examples out of the 46 TLS extracted from a friction experiment (see Figure S1 for an exhaustive presentation of the TLS). For each case, the TLS slowly emerges from the background noise, keeping a low waxing and waning amplitude. Some bursts or peaks in the signal occur randomly, creating some variability in the TLS. The maximum amplitude of TLS is always relatively small, in the range $\pm$ 5.10^{-7} $m.s^{-1}$. The apparent duration of a TLS is variable, with 90% of the records in the range 8-20 milliseconds. We compared the Fourier power spectrum of the acoustic events recorded during the experiments against the Fourier spectrum of background noise (Fig. 3). The acoustic event associated with a stick-slip event (see Fig. 1B for the time plot) presents a highly energetic spectrum with a few peaks between 10^4 and 10^5 Hertz. Conversely, the TLS spectrum is hardly above the noise spectrum in this same frequency range, confirming the low S/N ratio of these signals. Anyway, we can observe two peaks of energy at 48 and 57 kHz. The strong resonance inherent to the experimental set-up and the limited bandwidth of the sensor whose response is flat in the 10-60 kHz range probably alter the shape of the TLS spectrum. Nonetheless, most of the energy of the TLS apparently lies in the range 40-60 kHz. Such a frequency range corresponds to a wavelength of a few centimeters and indicates vibrations of the whole NaCl sample, and impairs the description of the microstructural process(es) at work during the emission of the TLS.

A continuous record of the acoustic emission together with the frictional force at a 500 kHz sampling frequency allows for a precise timing of the TLS with respect to the onset of slip acceleration. Doing such a careful analysis for all the recorded TLS we observe a systematic correlation between the onset of slip acceleration of the interface and the generation of TLS. Figure 2 exemplifies this behavior where the acceleration of slip (top plot) is associated with a burst of acoustic emissions (bottom plot) for the 4 selected slip events. There is a clear temporal correlation between the occurrence of TLS and the beginning of slip acceleration that starts when the shear stress equals the static resistance and the maximum level of dilatancy sustained by the slider is reached. The relation between shear stress level, dilatancy and tremor like signals might explain why the TLS progressively vanish while the slider is

still accelerating. We might infer from the experiments that the sliding of the interface is associated with a change in the contacts population resulting from the mass redistribution at the interface and leading to the generation of a TLS right before the drop in friction.

However, if slip acceleration is a necessary condition, it is not the only one to be met to emit a TLS. It is interesting to remark that TLS are not recorded at the beginning of the experiment, during the stick-slip stage (Fig. 1B). The interface has to accumulate some amount of slip before to emit TLS. This might be related to the restructuration of the sliding interface and the development of the striations parallel to the sliding direction [*Voisin et al.*, 2007; *Voisin et al.*, 2008]. A third condition has to be met, related to the state of stress and/or the peak dilatancy of the slider. TLS are not recorded randomly. During stage 2 (Fig. 1C), TLS are recorded only during the last smooth oscillation before the stick-slip, that is when the interface is close to failure. During stage 3 (Fig. 1D), TLS are recorded at each slip acceleration that occurs when the shear stress is at a maximum and starts to decrease gently. In both cases, the TLS occur at the maximum of the shear stress and also at the maximum of dilatancy bore by the slider.

Discussion and Conclusions:

TLS recorded in these experiments are related solely to the frictional process occurring along the contact interface. Because of the limited wavelength of the sensors used in this study, we are not able to characterize the processes at the origin of the TLS. Consequently, there is no simple possibility to derive a scaling between TLS and natural seismic tremors. Nonetheless, if we assume that the same process could produce seismic tremors in the nature as suggested by the coincidence of tremors with slow-slip events or by the fast migrations of tremors [*Brown et al.*, 2009; *Ghosh et al.*, 2009a; *Ide et al.*, 2007; *Kao et al.*, 2007; *La Rocca et al.*, 2009; *Larmat et al.*, 2009], we can use the laboratory results to shed some light on the natural system of slow slip, seismic tremors and triggering.

Result 1: This friction experiment conducted with a deformable interface exhibits a large variety of frictional behavior associated with different amounts of cumulative slip. These behaviors are themselves accompanied by different acoustic signals, impulsive events and TLS. A comparable variety of behaviors is observed on natural fault segments exhibiting in time and space different frictional behaviors: seismic, aseismic, creeping, associated with seismic events or seismic tremors.

Result 2: the TLS are emitted when the shear stress and/or the dilatancy are at maximum. A large and growing number of observations emphasize the link between stress changes and seismic tremors. Maybe the clearest evidence is the triggering of seismic tremor by large

transient shear stresses [*Rubinstein et al.*, 2007], dilatational stresses [*Miyazawa and Mori*, 2006], or the tidal modulation of tremor rate [*Rubinstein et al.*, 2008]. Such conveniently orientated stress waves temporarily increase the stress level on a given sliding interface or increase the dilatancy, inducing slip and tremor triggering like in the laboratory experiments. Another evidence might be found in silent or slow slip events that are often associated with seismic tremors in episodic tremor and slip events, described for the first time in Cascadia [*Dragert et al.*, 2001]. Tremors are sometimes found to migrate along strike, in agreement with the slow slip propagation [*Obara and Sekine*, 2009; *Shelly et al.*, 2007a]. Lead by the laboratory results, we propose that the temporary increase of stress induced by the rupture front propagation itself can trigger seismic tremors in zones where the stress state is close to its maximum. The present understanding of rupture propagation relies on a friction law, either slip-dependent or rate-and-state dependent, that defines a breaking-down zone governing the stress drop preceded by a short stress increase [*Ida*, 1975; *Rubin*, 2008; *Voisin et al.*, 2002]. Assuming that a similar breaking down process occurs for slow slip event, the small stress increase associated with the rupture tip would be able to trigger seismic tremors, according to our experimental results.

Result 3: TLS occur when the slider accelerates. Seismic tremors appear as a local recollection of the unstable frictional behavior occurring during the slippage of aseismic slow events down dip subduction zones [*Shelly et al.*, 2007a]. At a large scale, a slow slip event can be considered as an acceleration of slip on the interface during a few months, thus a possible source for seismic tremors. The slip complexity derived from inversion imposes slip rate variations and thus local accelerations that would be able to trigger seismic tremors.

Result 4: TLS are emitted only when enough slip is accumulated and the interface has developed a striation [*Voisin et al.*, 2007]. It is the case down-dip the subduction zones, where seismic tremors were first recorded. The recent discovery of the control of tremor migration by preferred directions linked to striation of the subduction plane [*Ide*, 2010] together with our experimental observations suggest that the striation is a necessary condition to emit seismic tremors and to control the tremor migration [*Ide*, 2010]. Large cumulative slips are also observed along some large continental strike slip faults. The relation between seismic tremors and seismic events in continental context remains open. If most of the seismic tremors and seismic events occur in different areas, the brittle crust for the latter, and the deeper ductile crust for the former, in very rare cases they do occur beneath the same location. It is the case with the Cholame area, a segment of the San Andreas Fault at the north tip of the great 1857 Fort Tejon earthquake rupture. Tremor activity was detected just before and after

the 2004 M6 Parkfield earthquake, at the depth where the earthquake rupture nucleated, at the transition between the stable sliding layer and the seismogenic layer [*Nadeau and Guilhem*, 2009] . Our experiment reported in Figure 1C shows that the same interface can generate tremors and seismic events. We observe that the TLS emission occurs systematically before the slip event. Because of the complete stress release in our experiment, the TLS rapidly stops after a few milliseconds. This is to be compared to the Cholame segment, where the "fore-tremor" activity was proposed before to the Parkfield earthquake of 2004. A recent study [Bouchon et al, Observation of Tremors Before a Large Earthquake, Science, in revision] also reports LFEs and tremors located in the hypocentral area before the large 1999 Izmit earthquake. We thus can imagine that the tremors would be generated by some creep acceleration eventually leading to the seismic event [*Shelly*, 2009]. If so, seismic tremors occurring at the base of the brittle crust might be seen as potential signature of the nucleation of seismic events.

Acknowledgments: This study was supported by ANR-09-JCJC-0011-01 grant. We acknowledge the technical support of Sophie Beauprêtre, Raphaël Jacquot, Adeline Richard, Sandrine Roussel, Benjamin Vial, and Liliane Jenatton. The authors thank Ruth Harris, André Niemejier and an anonymous reviewer for their constructive reviews.

References

Brown, J. R., G. C. Beroza, S. Ide, K. Ohta, D. R. Shelly, S. Y. Schwartz, W. Rabbel, M. Thorwart, and H. Kao (2009), Deep low-frequency earthquakes in tremor localize to the plate interface in multiple subduction zones, *Geophysical Research Letters*, *36*.

Burlini, L., G. Di Toro, and P. Meredith (2009), Seismic tremor in subduction zones: Rock physics evidence, *Geophysical Research Letters*, *36*.

Dragert, H., K. L. Wang, and T. S. James (2001), A silent slip event on the deeper Cascadia subduction interface, *Science*, *292*(5521), 1525-1528.

Dragert, H., K. Wang, and G. Rogers (2004), Geodetic and seismic signatures of episodic tremor and slip in the northern Cascadia subduction zone, *Earth Planets and Space*, *56*(12), 1143-1150.

Ghosh, A., J. E. Vidale, J. R. Sweet, K. C. Creager, and A. G. Wech (2009a), Tremor patches in Cascadia revealed by seismic array analysis, *Geophysical Research Letters*, *36*.

Ghosh, A., J. E. Vidale, Z. G. Peng, K. C. Creager, and H. Houston (2009b), Complex nonvolcanic tremor near Parkfield, California, triggered by the great 2004 Sumatra earthquake, *Journal of Geophysical Research-Solid Earth*, *114*.

Hirose, H., and K. Obara (2006), Short-term slow slip and correlated tremor episodes in the Tokai region, central Japan, *Geophysical Research Letters*, *33*(17), 5.

Ida, Y. (1975), ANALYSIS OF STICK-SLIP AND EARTHQUAKE MECHANISM, *Physics of the Earth and Planetary Interiors*, *11*(2), 147-156.

Ide, S. (2010), Striations, duration, migration and tidal response in deep tremor, *Nature*, *466*(7304), 356-U105.

Ide, S., D. R. Shelly, and G. C. Beroza (2007), Mechanism of deep low frequency earthquakes: Further evidence that deep non-volcanic tremor is generated by shear slip on the plate interface, *Geophysical Research Letters*, *34*(3), 5.
Kao, H., S. J. Shan, G. Rogers, and H. Dragert (2007), Migration characteristics of seismic tremors in the northern Cascadia margin, *Geophysical Research Letters*, *34*(3), 6.
Kao, H., S. J. Shan, H. Dragert, G. Rogers, J. F. Cassidy, and K. Ramachandran (2005), A wide depth distribution of seismic tremors along the northern Cascadia margin, *Nature*, *436*(7052), 841-844.
La Rocca, M., K. C. Creager, D. Galluzzo, S. Malone, J. E. Vidale, J. R. Sweet, and A. G. Wech (2009), Cascadia Tremor Located Near Plate Interface Constrained by S Minus P Wave Times, *Science*, *323*(5914), 620-623.
Larmat, C. S., R. A. Guyer, and P. A. Johnson (2009), Tremor source location using time reversal: Selecting the appropriate imaging field, *Geophysical Research Letters*, *36*.
Miyazawa, M., and J. Mori (2006), Evidence suggesting fluid flow beneath Japan due to periodic seismic triggering from the 2004 Sumatra-Andaman earthquake, *Geophysical Research Letters*, *33*(5).
Nadeau, R. M., and D. Dolenc (2005), Nonvolcanic tremors deep beneath the San Andreas Fault, *Science*, *307*(5708), 389-389.
Nadeau, R. M., and A. Guilhem (2009), Nonvolcanic Tremor Evolution and the San Simeon and Parkfield, California, Earthquakes, *Science*, *325*(5937), 191-193.
Obara, K. (2002), Nonvolcanic deep tremor associated with subduction in southwest Japan, *Science*, *296*(5573), 1679-1681.
Obara, K., and H. Hirose (2006), Non-volcanic deep low-frequency tremors accompanying slow slips in the southwest Japan subduction zone, *Tectonophysics*, *417*(1-2), 33-51.
Obara, K., and S. Sekine (2009), Characteristic activity and migration of episodic tremor and slow-slip events in central Japan, *Earth Planets and Space*, *61*(7), 853-862.
Peng, Z. G., J. E. Vidale, A. G. Wech, R. M. Nadeau, and K. C. Creager (2009), Remote triggering of tremor along the San Andreas Fault in central California, *Journal of Geophysical Research-Solid Earth*, *114*.
Peng, Z. G., J. E. Vidale, K. C. Creager, J. L. Rubinstein, J. Gomberg, and P. Bodin (2008), Strong tremor near Parkfield, CA, excited by the 2002 Denali Fault earthquake, *Geophysical Research Letters*, *35*(23).
Rubin, A. M. (2008), Episodic slow slip events and rate-and-state friction, *Journal of Geophysical Research-Solid Earth*, *113*(B11).
Rubinstein, J. L., M. La Rocca, J. E. Vidale, K. C. Creager, and A. G. Wech (2008), Tidal modulation of nonvolcanic tremor, *Science*, *319*(5860), 186-189.
Rubinstein, J. L., J. E. Vidale, J. Gomberg, P. Bodin, K. C. Creager, and S. D. Malone (2007), Non-volcanic tremor driven by large transient shear stresses, *Nature*, *448*(7153), 579-582.
Rubinstein, J. L., J. Gomberg, J. E. Vidale, A. G. Wech, H. Kao, K. C. Creager, and G. Rogers (2009), Seismic wave triggering of nonvolcanic tremor, episodic tremor and slip, and earthquakes on Vancouver Island, *Journal of Geophysical Research-Solid Earth*, *114*.
Shelly, D. R. (2009), Possible deep fault slip preceding the 2004 Parkfield earthquake, inferred from detailed observations of tectonic tremor, *Geophysical Research Letters*, *36*, 6.
Shelly, D. R., G. C. Beroza, and S. Ide (2007a), Complex evolution of transient slip derived from precise tremor locations in western Shikoku, Japan, *Geochemistry Geophysics Geosystems*, *8*.
Shelly, D. R., G. C. Beroza, and S. Ide (2007b), Non-volcanic tremor and low-frequency earthquake swarms, *Nature*, *446*(7133), 305-307.

Shelly, D. R., G. C. Beroza, S. Ide, and S. Nakamula (2006), Low-frequency earthquakes in Shikoku, Japan, and their relationship to episodic tremor and slip, *Nature*, *442*(7099), 188-191.

Thomas, A. M., R. M. Nadeau, and R. Burgmann (2009), Tremor-tide correlations and near-lithostatic pore pressure on the deep San Andreas fault, *Nature*, *462*(7276), 1048-U1105.

Voisin, C., I. Ionescu, and M. Campillo (2002), Crack growth resistance and dynamic rupture arrest under slip dependent friction, *Physics of the Earth and Planetary Interiors*, *131*(3-4), 279-294.

Voisin, C., F. Renard, and J. R. Grasso (2007), Long term friction: From stick-slip to stable sliding, *Geophysical Research Letters*, *34*(13), 5.

Voisin, C., J. R. Grasso, E. Larose, and F. Renard (2008), Evolution of seismic signals and slip patterns along subduction zones: Insights from a friction lab scale experiment, *Geophysical Research Letters*, *35*(8).

Figure Captions:

Fig. 1: (A) Sketch of the experimental block-slider system (details in supplementary material). (B, C, D) Frictional behavior of a salt/glass interface (top plots: recorded shear force divided by normal load, noted F/W) and associated acoustic emission records (bottom plots). (B) Typical stick-slip regime characterized by sudden shear stress drops separated by periods of stress accumulation. The acoustic emission is formed of large impulsive events, sometimes preceded and followed by smaller impulsive events. (C) The frictional behavior is more complex than previously. If the sudden jumps still occur, they are preceded by smooth oscillations of growing amplitude. This behavior is at the limit between stable and unstable behaviors. It arises with the cumulative displacement of the slider (here 3.3 mm; about 120 cycles) that modifies the properties of the salt interface. The associated acoustic emission presents a complex signal formed by a TLS with long duration (10 to 20 ms) and low amplitude followed by a strong impulsive and short duration event that represents the signature of the jump. (D) The frictional force remains more or less constant with small variations around a mean value (see insert): this is the stable regime obtained after 8mm (about 150 cycles) of cumulative slip. The associated acoustic emission is formed of a TLS with low amplitude and long duration, emitted at each slip acceleration, when the shear stress and the dilatancy are at maximum.

Fig. 2: Examples of TLS and the associated slip acceleration evolution. We present here 4 examples out of the 46 windows containing TLS. All TLS share some common features: progressive emergence from the background noise, very low amplitude, and rather long duration of 10-20 ms. Here and there, some bursts of energy create a variability of the TLS. Associated with the time traces of the TLS, we represent the shear stress evolution in a manner that mimics the slip acceleration. The high sampling rate of both force and acoustic emission and the short instrumental response of a millisecond allow for a precise comparison between acceleration of slip (top plot) and acoustic record (bottom plot). For each event A B C D, an arrow points to the beginning of slip acceleration determined by visual inspection. We note the strong correlation between the onset of slip acceleration and the emission of the TLS. The maximum of the TLS is reached after a few milliseconds. Note all TLS do occur at the beginning of the acceleration, and are thus associated with change of slip properties of the frictional interface.

Fig. 3: Fourier spectrums of the acoustic signature of a jump (blue curve), TLS (red curve), and noise (black curve) computed from 20 ms time windows. The low frequency range of the signals recorded below 10 kHz is not presented on the figure because it is dominated by experimental noise (motor) and associated with the movement of the slider as a block. The noise spectrum is computed from the mean of different time windows. The spectrum of a jump is highly energetic between 10 kHz and 100 kHz. By contrast the spectrum of the TLS is close to the noise level and presents only two clear peaks of energy at 48 and 57 kHz, not present in the power spectrum of the jump signal.

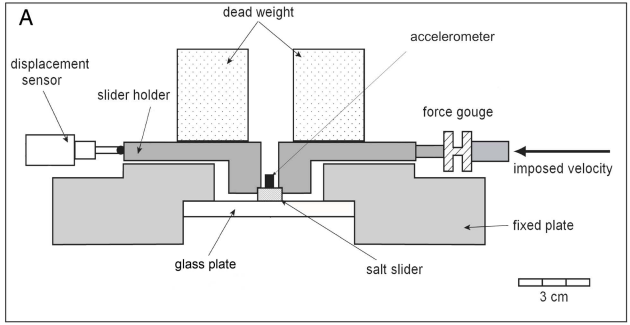
A
dead weight
accelerometer
displacement sensor
slider holder
force gouge
imposed velocity
fixed plate
glass plate
salt slider
3 cm

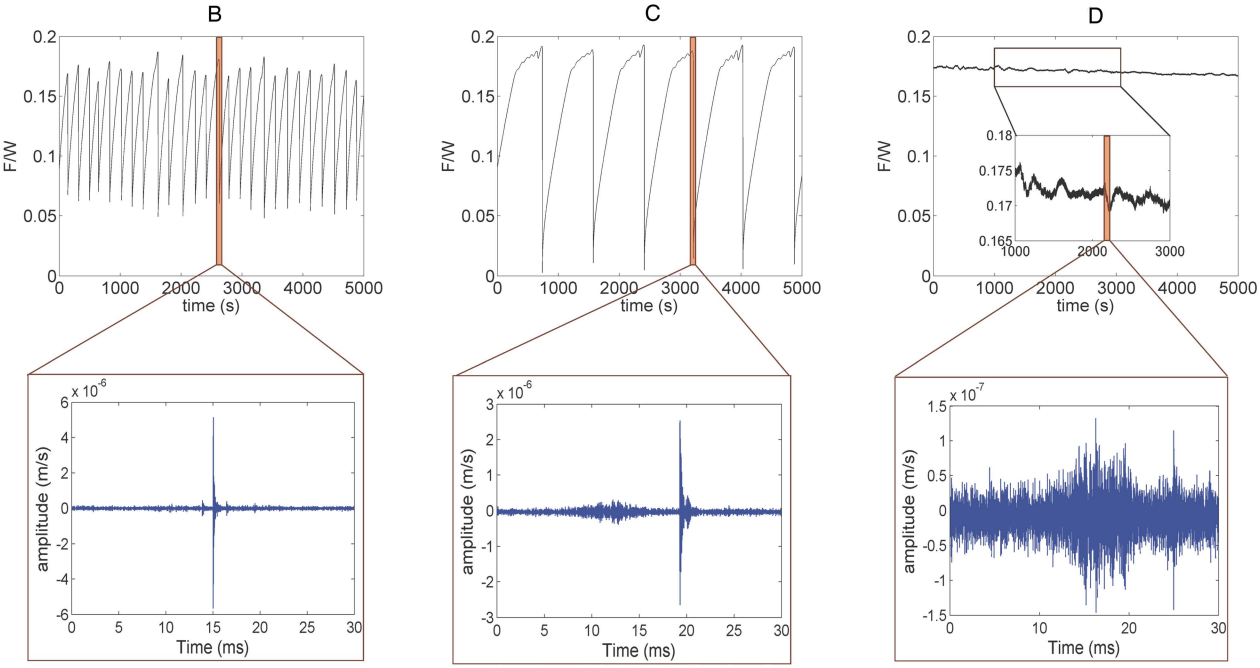
B
C
D
F/W
time (s)
amplitude (m/s)
Time (ms)
x 10^-6
x 10^-7

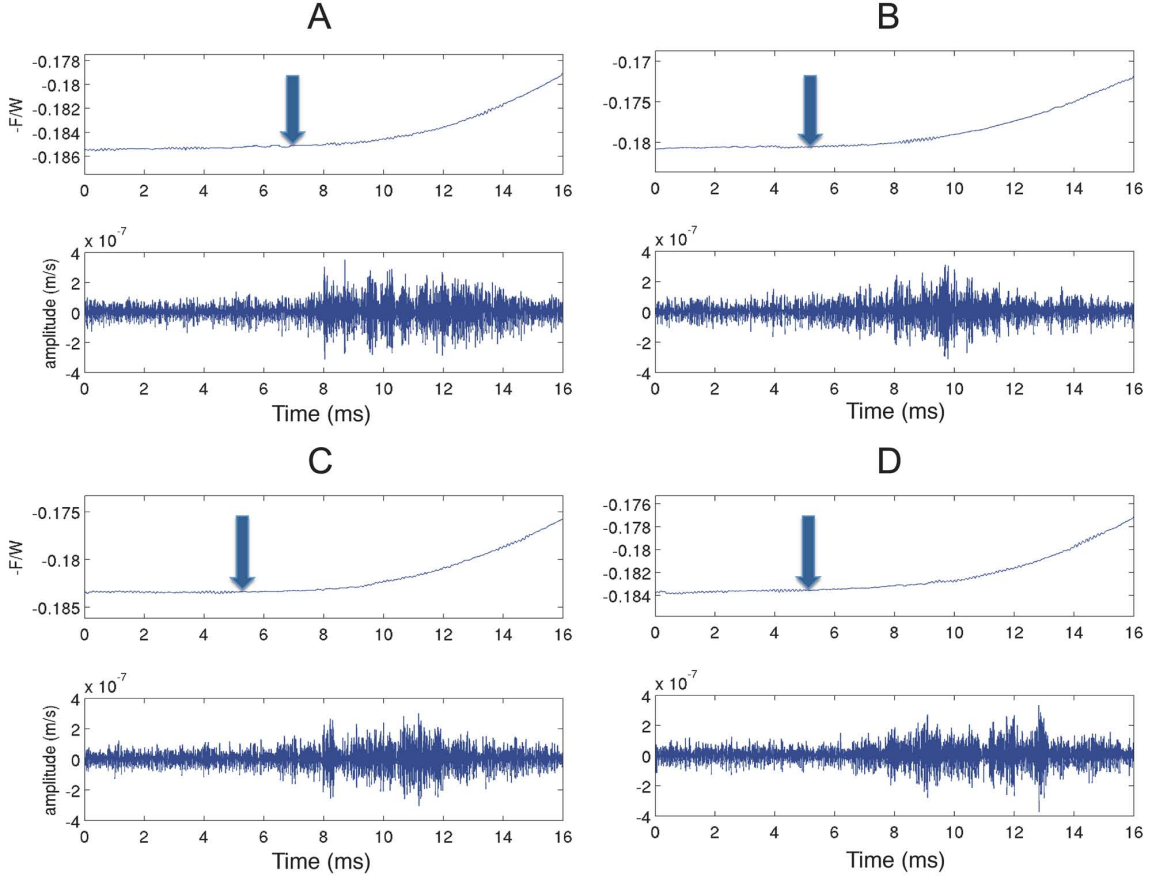
A
B
C
D
-F/W
amplitude (m/s)
x 10^-7
Time (ms)

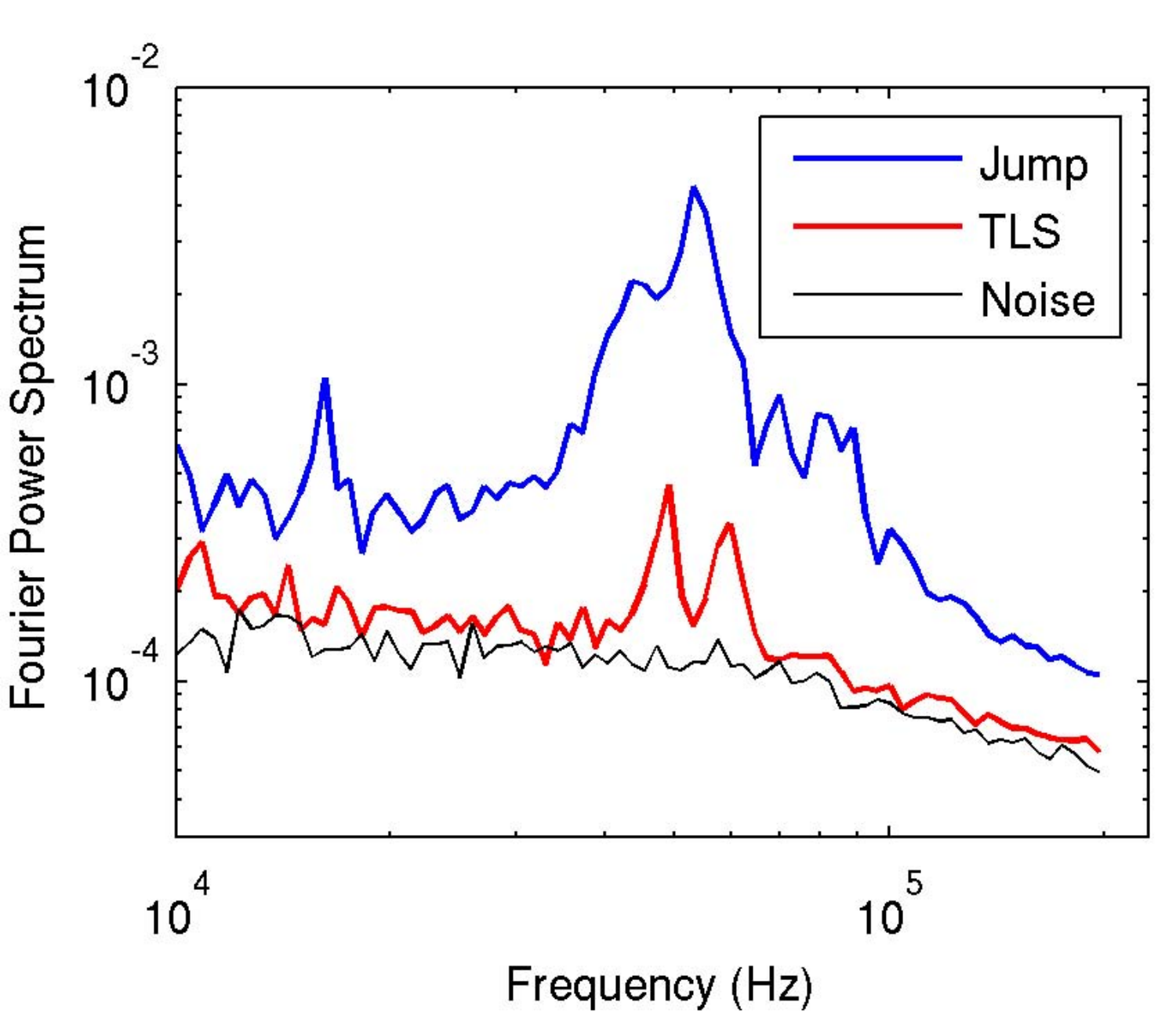
Jump
TLS
Noise
Fourier Power Spectrum
Frequency (Hz)
10^-2
10^-3
10^-4
10^4
10^5